International Journal of Nanoelectronics and Materials
IJNeaM
ISSN 198-5761 | E-ISSN 2232-1535

Development in Cell-Nanotopography Interaction Applications and Its Potential for Mass Production

Abdul Haadi Abdul Manap[a], Mohd Syakirin Rusdi[a], Siti Suhaila Md Izah[b] and Khairudin Mohamed[b,*]

[a]*Nanofabrication and Functional Materials (NFM) Research Group, School of Mechanical Engineering, Engineering Campus, Universiti Sains Malaysia, 14300 Nibong Tebal, Penang, Malaysia.*
[b]*Nano-Optoelectronic Research & Technology (NOR) Lab, School of Physics, Universiti Sains Malaysia, 11900 USM, Penang, Malaysia.*
**Corresponding author. Tel.: +04-5996321; e-mail: mekhairudin@usm.com*

ABSTRACT

Since the initial presentation of cell contact response with native topographic structure in 1911, numerous studies have been published to investigate how cells respond when interacting with micro/nano structures.. Many of the founding has potential to become applications in bio-medical or in pharmaceutical industry. Regardless of the huge prospect, these applications are still bound to the manufacturability of the micro/nano topographic structures. The introduction of nanoimprint lithography in 1995 has demonstrated that it can replicating micro/nano structures with relatively simple and low-cost equipment but with high throughput and high reliability. This paper reviews the development in cell-micro/nanotopographic interactions, the development of high throughput nanofabrication method. The nanofabrication methods in focus is nanoimprint lithography and electrospinning. This review paper also discusses the potential applications from cell-nanotopographic for mass productions. Prospectus applications such as the development in development of antimicrobial surfaces interactions and biologically inspired nanoscaffold and nanopattern suitable for tissue repair and regeneration are also discussed.

Keywords: *Cell, Nanotopographic, Nanoimprint*

1. INTRODUCTION

Advancements in nanofabrication have unveiled a multitude of possibilities for the interaction between cells and nanotopography. According to Robert Langer's research, nanotechnology has the potential to revolutionize and reshape the biomedical and pharmaceutical sectors.[1]. The nanotechnology market in healthcare and medicine is estimated to grow to more than USD334 billion by 2025 [2].
In order to tackle potential applications that leverage cell-nanotopography interactions, there is a need to create cost-effective and efficient techniques for nanofabrication Several ideas have been introduced and developed for high throughput nanofabrication. Methods relying on direct mechanical deformation, like nanoimprint lithography (NIL), are crucial in the nanotechnology-driven medical and pharmaceutical sectors due to their cost-effectiveness, repeatability, and efficiency.[3], [4].

Cells typically exist at the micro scale, and the initial exploration of cell responses to native topographic structures was conducted by Harrison in 1911 [5],[6]. Remarkably, when a cell interacts with a surface featuring dimensions smaller than itself, it exhibits a distinct response, e.g., structure on nanostructure. Cell respond in many ways with nanostructures and some of those responses are useful, and these interactions can be utilized as tools to direct the cell responses[7]–[12]. Nanostructure that interacts with cells can be used as mechanosensory to transmit signals for cell adhesion, proliferation and differentiation[7]–[12]. Understanding the interaction between cells and nanotopographic structures is primarily contingent on knowledge about cell adhesion[13]. If the cell fails to adhere to the surface, other responses become irrelevant. Numerous studies have explored various types of nanotopographic structures in this regard. Cell interactions with nanotopography can be categorised into three groups, namely cell with precise and highly symmetrical nanostructures[14], [15], cell with randomize nanostructure[16], and cell with disorder nanostructure[17]. This paper reviews the history and recent development of these three categories.

2. CELL-MIRO/NANOTOPOGRAPHY INTERACTION

Numerous investigations have been undertaken to delve into stem cells, examining their interactions with nanotopography [18]. The main objective of research in stem cell is to control the differentiation of stem cells into specific cell lineages. Utilizing the interaction between mesenchymal stem cells (MSCs) and nanotopography can serve as a means to regulate their differentiation [18]–[21]. When placed on nanotopography, human embryonic stem cells (hESCs) exhibit a similar interaction. The nanotopological mechanosensory of hESCs has noteworthy effects on cell spreading, adhesion, and self-replication

[22], [23]. The interaction between human embryonic stem cells (hESCs) and nanotopography holds significant potential in the realms of tissue engineering and medical applications. This is attributed to the distinctive characteristics of hESCs, particularly their pluripotency, which allows them to differentiate into various specialized human cells [24], [25]. Numerous investigations have been carried out to analyze cell interactions with TiO2 nanotubes. Cellular responses, such as adhesion, proliferation, and apoptosis, are contingent on the size of the nanotube. Park et al. [26]showed that indicates that cell adhesion and proliferation reach their peak on nanotubes with a diameter of 15 nm, while apoptosis occurs at a diameter of 100 nm. Numerous studies align on the consensus that the fate of cells is determined within the threshold nanotube size of 30-50 nm [25]. Surfaces featuring nanotube diameters exceeding 50 nm can lead to cell impairment, restricting both cell spreading and adhesion, irrespective of the specific surface characteristics [27], [28]. Although large nanotubes (diameter >50 nm) impair cells from spreading and adhere, they evoke stem cells to elongate[29], [30] The elongation of mesenchymal stem cells (MSCs) induces a change in cytoskeletal structure, driven by a heightened tension state. This alteration subsequently results in the generation of osteoblast-like cells [30]–[32]. This breakthrough unveils a new avenue for advancement in nanotechnology, particularly in the field of orthopedic treatment.

Regarding the selection of nanotopography, three nanostructure options are available. The initial approach involves investigating cell interactions with symmetric and highly precise nanostructures [14], [33], [34]; The second approach entails examining cell interactions with randomly textured nanoscale roughness [16], [35] and the third approach involves adopting a middle ground between precision and randomness, known as disorder nanotopography [18]. When cells interact with precise nanotopography, the typical outcome is lower cell adhesion compared to interactions with random nanoscale roughness [14], [16], [34], [36]. Interestingly, McMurray et al. [37] stated that precisely symmetrical arrangement of nanopits has been demonstrated to maintain the phenotype and multipotency of hMSCs over an extended period, lasting up to eight weeks.

On the other hand, Dalby et al. [17] showed that the contact between disordered nanotopography and mesenchymal stem cells (MSCs) leads to swift osteogenesis, comparable to the outcomes achieved using corticosteroids such as Dexamethasone as agents inducing bone formation. Table 1 present the collection of studies in cell responses to precise and highly symmetric nanostructures, Table 2 present the collection of studies in cell responses to randomize nanostructures and Table 3 present the collection of studies in cell responses to disorder/irregular nanostructures.

Table 1 Collection of studies in cell response to precise and highly symmetric nanostructures

Structure Type	Substrate Material [b]	Cell Type [a]	Feature size	Adhesion	Proliferation	Elongation, alignment [c]	Other [d]
Nanogrooves (Gong et al. 2015a; Ozguldez et al. 2018) [38], [39]	PUA co-culture with HUVECS	hMSCs	a. Space Gap = 550nm, 1650nm and 2750nm b. Width = 550nm	hMSCs and HUVESC fully adhered the substrata.	There is no notable difference with a flat substrate.	hMSCs and HUVESC aligned with the nanopattern exhibit a CEF 2-3 times greater than that observed on a flat surface.	Osteogenesis highest at space gap 1650nm.
Nanograting (Yang et al. 2017) [40]	PDMS	hMSCs	a. Pitch = 700nm and 1µm b. Depth = 350nm c. Width = 350nm and 500nm	Culturing hMSCs on nanogratings results in a decrease in integrin subunits.	-	On nanogratings, hMSCs align and elongate, whereas on a flat surface, cells spread randomly.	Substrate stiffness and topography impact both hMSCs' focal adhesions (FA) and F-actin.
Nanopillar and nanowell (Muhammad et al. 2015) [41]	TCPS coated with FNC or LC	HCECs	a. d = 1.38µm wells b. d = 356nm pillar c. d = 1.80µm pillars	-	Every substrate demonstrates a higher proliferation rate compared to the plain surface. Especially, HCECs on 1µm FNC-coated pillars exhibit a considerably increased proliferation , with a 2.9-fold	HCECs exhibit elongation in p-media , while in s-media, the cells become fully confluent and maintain their native shape.	Nanotopographic memory aids HCECs in maintaining functional markers.

					difference.		
Nanopost (Gong et al. 2015b) [38]	PUA	hMSCs	a. Spacing Gap = 1.2 µm, 2.4 µm, 3.6 µm and 5.6µm b. d = 700nm	The surface contact area of hMSCs decreases when exposed to denser nanoposts.	-	-	Higher nanopost density favors osteogenesis in hMSCs, while lower nanopost density promotes adipogenesis.
Nanograting (Antonini et al. 2016; Donnelly et al. 2018) [42], [43]	PET	hMSCs	a. Depth = 350nm b. $Width_{ridge}$ = 500nm and 1µm c. $Width_{groove}$= 500nm and 1µm	Nanogratingdoes not affect hMSCs adhesion.	At 24 hours and 72 hours of experiments, no significant apoptosis or necrosis were measured.	Cell area reduction was observed at PET with nanogrooves and nanoridge of 500nm. hMSCs on both sample elongated and differentiate into osteoblastic cells.	PET shown to have mechanotransduction property apart of its biocompatibility.

[a] hMSCs = human mesenchymal cells ; HCECs = human corneal endothelial cellls[b] PUA=Polyurethene acrylate, HUVECS = human umbilical endothelial cells ; PDMS = Polydimethylsiloxane; TCPS = Tissue Cultured Polystyrene ; FNC = mixture of fibronectin and collagen ; PET = polyethylene terephthalate[c] CEF = cell elongation factor [d] FA = Focal Adhesion; LC = laminin (Gibco) and chondroitin sulfate (Sigma) mixture

Table 2 Collection of studies in cell response to randomized nanostructures

Structure Type	Substrate Material [c]	Cell Type [b]	Feature size [a]	Adhesion	Proliferation [d]	Elongation, alignment	Other [e]
Nanoroughness (Murali et al. 2021) [44]	Glass coated with vitronectin	hESCs	R_q between 1nm to 150nm	Decrease with R_q increase.	Doubling time increase with R_q increase.	hESCs on high R_q are more compact and shorter cytoplasmic extension.	hESCs differentiation increase on rough surface.
Surface featuring microfibers with elliptical-shaped nanopores. (Zhou et al. 2015) [45]	PLLA mircrofiber with nanopores surface	vSMCs	a. $AR_{ellipse}$ = 2.7-3.9 (54.8 – 110.0nm) b. d_f = cs. 1.6µm	After 8 hours cultured, the number of attached vMSCs increased.	After 7 days, cultured, PLLA fiber shown to support cell proliferation	After 8 hours cultured, cell elongated	The nanopores on the microfiber surface enhances cell bio-mimicry, fostering the synthesis of vascular protein matrix proliferation and enhanced adhesion.
a. Cylindrical microfiber with smooth (CS) b. Cylindrical microfiber with porous (CR) surface c. Ribbon microfiber with smooth (RS) and porous (RR) surface (Lopez Marquez et al. 2022) [46]	PLGA	NCs	a. $R_{q(CR2)}$ =182nm b. $R_{q(CS)}$ = 170nm c. $R_{q(RR2)}$ = 363nm d. $R_{q(RS)}$ = 366nm e. $R_{q(CR1)}$ = 418nm f. $R_{q(RR1)}$ = 160nm	Rough fibre increase adhesion.	The roughness parameters obtained exhibit a correlation with cell proliferation. Linear model of cell proliferation is formulated from five roughness parameters S_p,S_{sk},S_q,S_m and S_a.	-	The scaffold made from PLGA does effect the toxicity level within the culture medium.
Nanoroughness (Delaine-Smith et al. 2021) [47]	Ti	hMSCs	R_c = 22nm	-	-	-	The upregulation of a specific marker, comprising 20 miRs, is twofold higher in hMSCs when cultured on titanium with nanoroughness. This finding indicates that the chemical induction of nanoroughness on the titanium surface encourages osteogenesis.
Precise spatially nanoroughness	Glass	NIH/3T3	R_q between 1nm to 150nm	NIH/3T3 adhere at	There is a significant	-	Nanotopography induces cell

(W. Chen, Sun, and Fu 2013) [48]				glass with R_q = 70nm.	increase in proliferation on rough surfaces		mechanosensitivity, consequently reducing NIH/3T3 cell contractility in the cytoskeletal (CSK).
Nanopit (Stewart 2019) [49]	Polycarbonate	MSCs	a. d = 120nm b. depth = 100nm	-	-	-	Osteoblastogenesis occurs through two distinct mechanisms: one induced by nanotopography and the other through piezo-stimulated mechanotransduction.

[a] R_q = rot-mean-square roughness ; d_f= fiber diameter ; $AR_{ellipse}$= Ellipse-shaped aspect ratio[b] vSMCs = vascular smooth muscle cells;hESCs = human embryonic stem cells ;; NCs = Nerve Cells ; NIH/3T3 = mouse embryonic fibroblast cells; MG-63 = osteoblast-like-cell ; hFOB = human fetal osteoblast [c] PLGA = poly(lactic-co-glycolic acid) ; PLLA = poly($_L$-lactic acid) ;Ti = Titanium; YSZ-(110) = (110) oriented yttria-stabilized zirconia single crystal ; GDC = gadolinium-doped ceria [d] S_p= Maximum height ; S_{sk}= Height distribution deviation ; S_q= Root mean square deviation ; S_m = Peak material volume ; S_a = Arithmetic mean deviation [e] CSK = Intracellular actin cytoskeleton

Table 3 Collections of cell response to disorder/irregular nanostructure

Structure Type [a]	Substrate Material [c]	Cell Type [b]	Feature size	Adhesion	Proliferation [d]	Elongation, alignment	Other
Nanopit (Pemberton et al. 2015) [50]	Polycarbonate	MSCs	a. d = 120nm b. depth = 100nm	-	-	-	Osteoblastogenesis takes place through two distinct mechanisms, one induced by nanotopography and the other through piezo-stimulated mechanotransduction.
RGD nanopattern (Choe et al. 2022; Sun et al. 2022) [51], [52]	Glass	MC3T3-E1	a. Spacing = 55-101 nm b. h_{RGD} = 10nm	Cell adhesion is superior on a disordered nanopattern compared to an ordered nanopattern. This is attributed to the wider range of ligand density present in the disordered nanopattern.	-	-	Integrin clustering and adhesion through RGD ligands occur when the spacing between ligands is larger than 70nm.
Nanotube (Oh et al. 2009) [53]	Ti	hMSCs	d = 30, 50, 70, 100nm	a. The quantity of adhered cells exhibits an inverse relationship with the size of the nanotubes. b. Nanotubes with a diameter of 30nm facilitate cell adhesion without inducing differentiation.	-	Larger diameter nanotube promote osteoblastic differentiation.	There is an inverse relationship between cell adhesion and cell elongation.
Nanopit (5 Patterns / Arrays) 1. SQ 2. HEX 3. DSQ50 4. DSQ20 5. RAND (Nakamoto et al. 2022) [54]	PMMA	Osteoprogenitors MSCs	a. d = 120nm b. depth = 100nm	a. MSCs on DSQ50 show longer adhesion compare to SQ and HEX that have poor adhesion. b. Osteoprogenitor loss adhesion on HEX.	a. MSCs proliferation on DSQ50 significantly higher than MSCs on planar substrate with DEX. b. Osteoprogenitors on DSQ50 formed dense	a. After 21 cultured, MSCs on SQ show fibroblastic appearance and on RAND show osteoblastic appearance. b. MSCs on DSQ20 show significant osteoblastic	MSCs osteogenesis were rapidly induce by interact it with controlled nanodisorder.

					aggregate and form bone nodul structures. c. Number of osteoprogenitors decreases on SQ.	morphology. c. Osteoprogenitors on DSQ50 formed bone nodul structures after 21 days cultured.	

[a] RGD = arginine glycine-aspartic acid SQ = square Array ; HEX = hexagonal array ; DSQ20 = disordered square array with dots randomly displaced by up to 20 nm along both axes from their positions in a true square; DSQ50 = disordered square array with dots randomly displaced by up to 50nm along both axes from their original positions in a perfectly square arrangement. ; ; RAND = pits placed randomly over a 150 μm X 150 μm field, repeated to fill a 1 cm^2 area [b] MSCs = Mesenchymal Cells; MC3T3-E1 = mouse osteoblastic cell line [c] PMMA = polymethylmethacrylate [d] DEX = dexamethosane

To harness the interactions between cells and nanotopography, a comprehensive understanding of cell adhesion is likely the most crucial aspect. Cells that adhere to surfaces through cellular adhesion receptors are known as integrins. Cells exhibit distinct responses to variations in mechanical force [18], surface topography[19] and surface chemistry[55]. In describing cell adhesion, Dalby et al. [13] provided an analogy, a cell can be likened to a tent, where the pegs represent integrin clusters serving as anchors that secure the tent to the ground. Nevertheless, cells have the ability to determine the location of integrin clusters by modifying their cytoskeleton. When a surface features a nanostructure with dimensions similar to those of the cell's integrin, signals can be relayed to the cell via the integrin

Cells cannot interact directly with any synthetic material. Instead, it can adhere to the protein layer adsorbed on the material surface[62]. Cell adhesion can be studied using the spatial organization of arginine-glycine-aspartic acid (RGD) ligands[64]–[66]. In a previous study, Cavalcanti-Adam et al. [67] produced a threshold density (70 nm) for the RGD spacing for the focal adhesion to be formed. Cell adhesion decreases significantly when the RGD spacing is greater than 67 nm[68]–[70].

3. DEVELOPMENT IN NANOTOPOGRAPHY FABRICATION

The integral part of shifting the application of cell-nanotopography interaction from laboratory to industrial scale is the nanotopography fabrication. There are many methods for fabricating nanostructure from

random fabrication to precise fabrication. The applications of these methods are attributed to many factors such as cost, precision, repeatability and many more. Randomize method, such as blasting, can produce nanostructures more easily, while top down fabrication techniques, such as reactive ion etching and electron beam lithography has the capability to achieve features as small as 10 nm. [71]. Although precise techniques yield more controlled and consistent outcomes in contrast to random methods, they often entail higher costs and require expertise to attain the desired nanostructure.[72],[73]. Moreover, these methods are labor-intensive and time-consuming, rendering them impractical for large-scale production. To stimulate innovation and propel research in cell-nanotopography technology, it is essential to develop low-cost, high-throughput, and high-resolution nanolithography techniques nanolithography[74]. The rapid progress in the semiconductor industry has notably hastened the development of micro/nanofabrication techniques. Innovations like nanoimprint lithography (NIL) and electrospinning now empower researchers to construct and fabricate nanostructures on larger substrates at a more cost-effective rate[75]. NIL was first introduced by Chou in 1995 [76] demonstrating promising potential to offer a cost-effective and high-throughput method for producing continuous high-resolution nanostructures [77]. In NIL, the mold created is transferred onto a resist using specialized printing equipment [78]. In this approach, the master mold is generated through precise fabrication techniques, such as focused ion beam or electron beam lithography [79]. The nanostructure can be replicated repeatedly by imprinting it onto a suitable substrate.

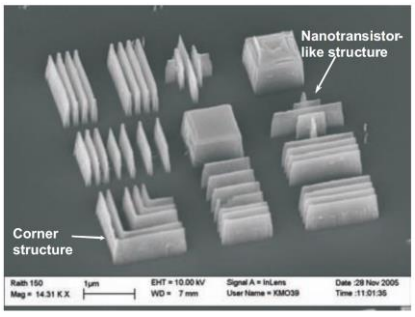

Figure 1. SEM images of 60nm features on quartz substrate [73].

Figure 2 depicts a difference between two types of nanoimprint Lithography (NIL) which are thermal NIL and ultraviolet (UV) NIL. In thermal NIL, the mold used for imprinting is heated just beyond the glass transition temperature, T_g of the resists. The elevated temperature softens the resist, allowing it to fill the cavities and create a reverse pattern of the mold. Subsequently, the mold is cooled to a temperature below the glass transition temperature, T_g of the resist before being disjointed. In UV NIL, the entire process, including resist UV-curing and the demolding process, is carried out at room temperature, eliminating the need for elevated temperatures. [81]. Unlike thermal Nanoimprint Lithography (NIL), which depends on phase changes corresponding to temperature adjustments, UV NIL induces resist hardening through increased cross-linking

in UV-sensitive polymer [82]. UV NIL necessitates smaller imprint pressure compared to thermal NIL because it employs a less viscous photoresist. .In addition to UV NIL and thermal NIL, there are also variants of Nanoimprint Lithography (NIL) that combine both UV and thermal curing, such as (STU®) imprint technology by Obducat Technologies [85]. These techniques allow the Nanoimprint Lithography (NIL) cycle to be carried out at a constant temperature by simultaneously employing both thermal curing and UV curing. NIL based on imprint contact encompasses three variants: roll-to-roll (R2R), plate-to-plate (P2P) and roll-to-plate (R2P), Figure 3 shows the differences between these three NIL methods. In terms of potential for mass production, R2R NIL holds significant promise for industry-scale applications. The R2R NIL concept is rooted in roll-to-roll manufacturing processes, enabling the continuous and high-throughput production of products.[86], [87]. Roll-to-roll (R2R) NIL presents greater advantages compared to conventional plate-to-plate (P2P) NIL in terms of equipment size, imprint force and output. [88]. Wong et al. [89] has successfully demonstrated the double-sided R2R NIL which able micro or nanostructure imprinted to both side of targeted substrate. Table 4 present the collection of studies and research that using different type of NIL

Another method for producing inexpensive, relatively easy and high throughput nanostructures is electrospinning[79]. Electrospinning has been used for mass production for decades. However, this method is not preferred compared to other spinning methods due to its lower production rate. As a result, many studies have been conducted to improve electrospinning. For instance, the Karpov Institute of Physical Chemistry used swirling air jet to form multiple solution-spinning jet[95]. A study conducted in Korea using cylinder-type multi nozzle electrospinni system showed great potential for mass production of nanofibers[96].

Cellular responses to molecular-scaled structures in contact surfaces were first proposed in 1963 by Rosenberg[97]. However, it was in 1999 when Laurencin et al. [98] reported that fibroblastic cells are adhered and realigned properly with fibers with a diameter smaller than the diameter of the cell. Numerous research have been done to investigate the behavior of cells when interacting with nanofiber scaffolds. Electrospinning is a simple method to produce nanofibrous scaffold for cell- nanotopography interactions. Electrospinning was first introduced and patented by Formalas in 1934[99]. Prior to that, researchers focused on electrospinning as a method to produce fibers which are used to reinforce composite materials, thereby improving mechanical properties[100]. Figure 4 shows the schematic set up to produce uniaxial nanofibers.

Table 4 Collection of studies that using different technique of NIL

Researcher	NIL Type	Mold	Resist	Final Product	Resolution
Y. Chen et al. 2021 [90]	P2P	SiO_2 (quartz) template	Polystyrene	Sub-10nm width ribbon of hexaganol graphene nanomesh (GNMS).	Sub-10 nm of ribbon width.
Potejanasak 2021	P2P	SiO_2 (quartz) template	TR-21 from Tokyo Gosei Co. Ltd.	120 nm diameter of CoPt nanodots.	120 nm diameter of nanodot.
Ye et al. 2010 [91]	P2P	Hydrogensilsesquioxane(HSQ)	Polyset® epoxy siloxane nanoimprint resist from Polyset Company Inc., Mechanicville, New York, USA	50nm lines and dot with high aspect ratio are succuesfully replicated using PDMS soft mold.	sub-100 nm of periodic nanoline and array of nanodot.
Sousa et al. [92]	R2P	Thin Ni film	PMMA	Sub-100 nm of PMMA nanogratings.	Sub-100 nm of nanograting.
Ahn and Guo 2009 [86]	R2P	Ethylene Tetrafluoroethylene (ETFE)	Epoxysilicone	300 nm line width and 600 nm of epoxysilicone nanogratings.	300 nm line width of nanograting.
Schleunitz et al. 2011[75]	R2R	OrmoStamp coated with antisticking layer (ASL)	Celluose Acetate (CA) film	200 nm depth and width of CA. (A continous 40 m of CA printed).	200 nm line width of nanograting.
Nagato et al. 2010 [93]	R2R	Si(Silicon) template	PMMA	Multilayer nanograting with 800nm pitch.	300 nm depth of multilayer nanograting.
Lee et al. 2018 [94]	R2R	Polyurethane acrylate	PDMS	Gecko-foot-inspired hierarchical nanostructure.	
Wong et al. 2018 [89]	R2R	UV-curable resin	PDMS	Micro-nano structure fabricated/imprinted on both side of targeted substrate (double sided).	200nm nanopore.

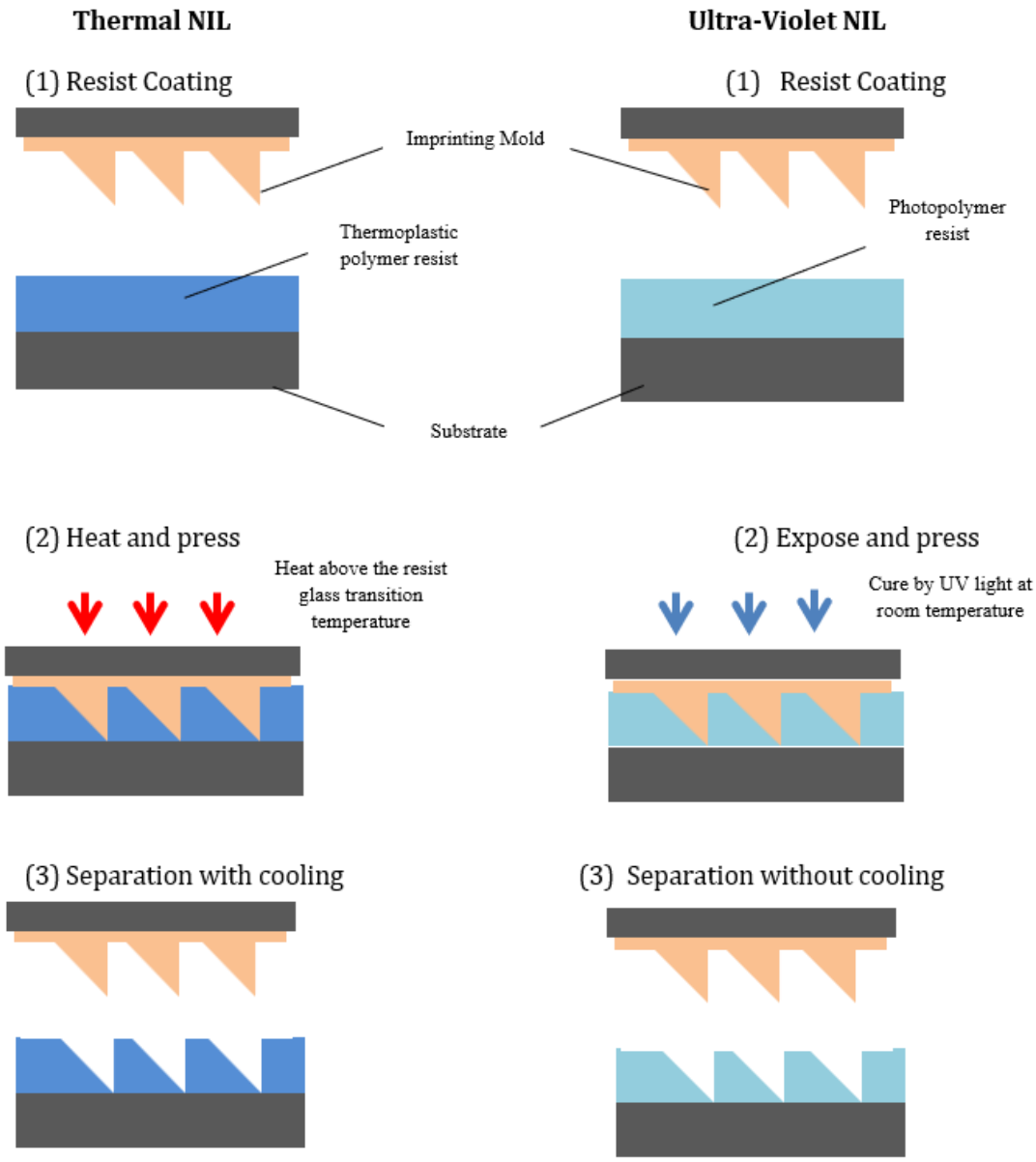

Figure 2. Comparison between Thermal NIL and Ultra-Violet NIL.

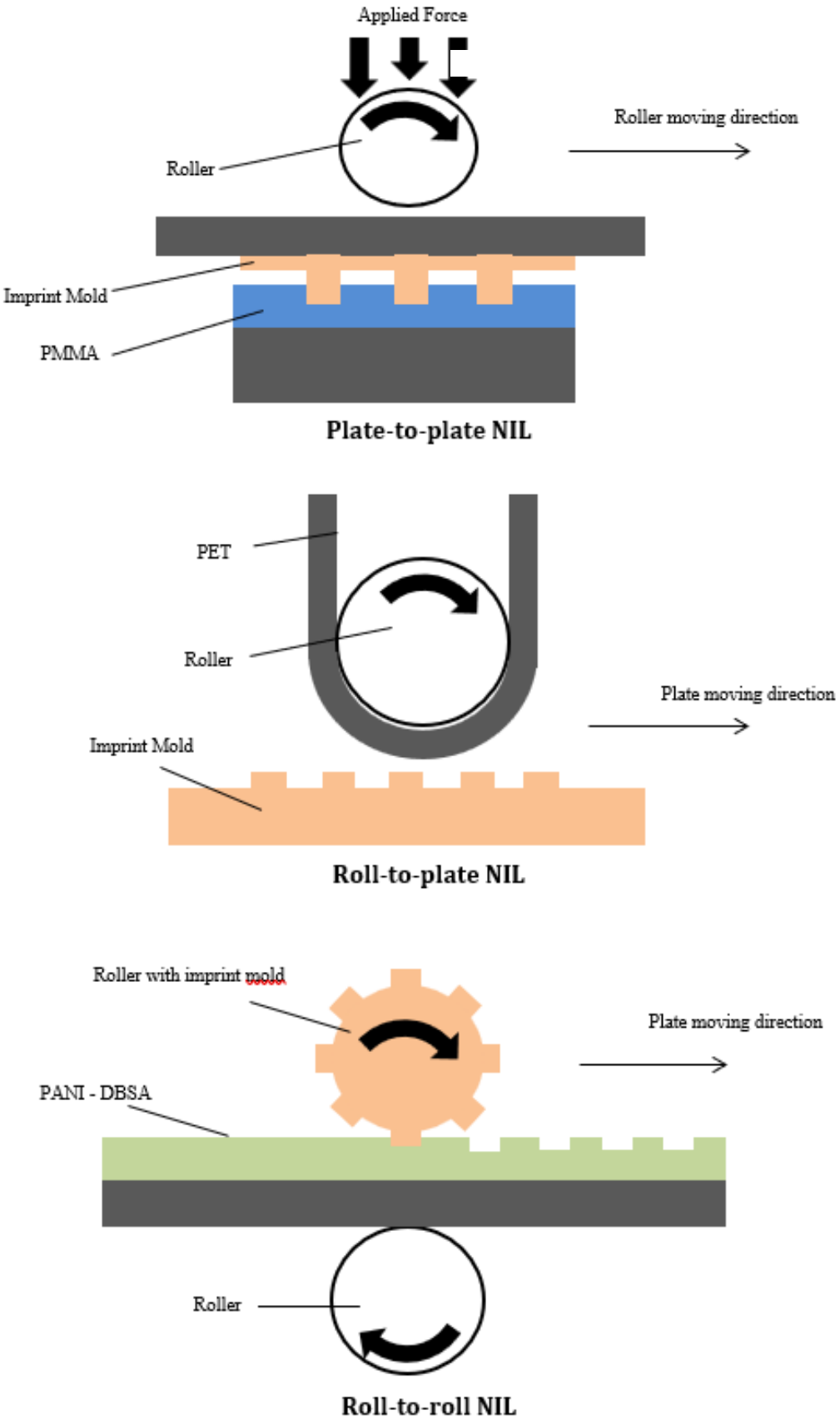

Figure 3. Nanoimprint lithography variation based on imprint techniques.

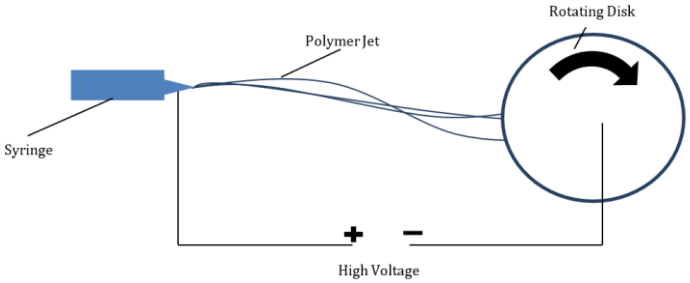

Figure 4. Schematic set up of electrospinning to collect uniaxial nanofibers.

When a high voltage is applied between the conducting syringe and conduction collector (i.e., rotating disk), the voltage bias will convert the polymer droplets on the syringe needle into a polymer jet. Nano-sized polymer jets are collected by rotating disk producing uniaxial nanofibers. The final product can vary by changing collectors. The rotating disk collector will produce uniaxial nanofiber, plate collector will produce random nanofiber, and rotating drum collector can produce uniaxial nanofiber. Random nanofiber are produced depends on the bias voltage.

Table 5 Summary of various studies that using different material and collector for electrospinning

Researcher	Collector Type	Material	Fiber Diameter	Specification
Nasouri et al. (2012) [101]	Rotating drum for random nanofiber	PAN/DMF	80-162nm	Flow rate: 0.25mL/h Voltage: 25kV Distance: 12cm
Yu et al. (2014) [101]	Flat plate for random nanofiber	Collagen/PCL/ Choloroform/CNTs	564nm	Flow rate: 2mL/h Voltage: 16kV Distance: 12cm
Zhu et al. (2015) [102]	Parallel metal plates for aligned microfiber	Collagen/silk/HFIP	1-2μm	Flow rate: 5mL/h Voltage: 15-25kV Distance: 10-20cm
Cho et al. (2016) [103]	Rotating custom-made drum for random/aligned nanofiber	PCL/DCM/DMF	750-1000nm	Flow rate: 1mL/h Voltage: 14-16V Distance: 19cm
Johnson et al. (2016) [104]	Rotating disc for aligned microfiber	PLLA/Chloroform	170-200μm	Flow rate: 2mL/h Voltage: 10kV Distance: 5cm
Roman et al. (2016) [105]	Rotating disc for aligned microfiber	PlLA/Chloroform/DMF	1.36-1.56 μm	Flow rate: 1.1mL/h Voltage: 10V Distance: 10cm
Shafei et al. (2017) [106]	Rotating drum for random nanofiber	PCL/DMF/Tetrahydrofuran	450-1150nm	Flow rate: 2mL/h Voltage: 13kV Distance: 20cm

4. CELL-NANOTOPOGRAPHY APPLICATIONS FOR MASS PRODUCTION

The cellular reaction to the nanostructure can be harnessed for various applications. One such application that can leverage this cellular response is the development of antimicrobial surfaces. Similar surfaces can be found naturally in dragonfly wing [107] and gecko skin [108] and researcher around the world try to replicate these surfaces in antimicrobial As an example, research conducted by Ivanova and her colleagues revealed that dragonfly wings, characterized by nanocones with dimensions of 50-70 nm in base diameter and a height of 240 nm, exhibit distinct antibacterial properties. [107]. In another study by Kelleher et al., it was observed that the nanopillars present on cicada wings demonstrate effective antimicrobial properties against gram-negative bacteria, specifically Pseudomonas aeruginosa [109]. Table 6 summarized the list of artificial nanostructured bactericidal surfaces with their preparation method. The table exhibits the artificial antibacterial surfaces with various patterns such as silicon-based surfaces, titania-based surfaces and flexible polymer surfaces. These

artificial antibacterial surfaces were fabricated with different preparation methods such as RIE, hydrothermal process, anodization, thermal oxidation, NIL, direct laser interference patterning and EBL technique.

Table 6 Summary of various bio-inspired studies for bactericidal surfaces

Researchers	Surface	Preparation method	Surface features and size	Bactericidal activity
Hasan et al. (2015) [110]	Black silicon	DRIE	Nanograss Diameter 220 nm Height 4000 nm	Lethal to *E-coli* and *S-aureus*
Fisher et al. (2016) [111]	Diamond nanocone surface	RIE	Nanocones Width 0.3-1.2 μm Height 3500 nm	Lethal to *P-aeruginosa*
May et al. (2016) [112]	Diamond coated black silicon	RIE	Nanoneedles Height 0.5-1.4 μm Height 15-20 μm	Lethal to *P-aeruginosa*
Bhadra et al. (2015) [113]	Titanium nanopatterned arrays	Hdrothermal process	Nanopatterned arrays Diameter 40.3 nm	Effective killing *P-aeruginosa,* Less lethal *S-aureus*
Hizal et al. (2015) [114]	Ti alloy nanospike surface	Anodization	Nanospikes Diameter 100 nm Spacing 2 μm Height 2 μm	Lethal to *S-aureus*
Sjostrom et al. (2016) [115]	Ti alloy nanospike surface	Thermal oxidation	Nanospikes Diameter 20 nm	Lethal to *E-coli*
Dickson et al. (2015) [116]	Nanopatterned PMMA surface	NIL	Nanopillar Diameter 70-215 nm Height 200-300 nm	Lethal to *E-coli*
Kim et al. (2015) [117]	Nanopatterned PMMA film	NIL	Nanospores Depth 460 nm Spacing 300 nm	Restricted attachment of bacterial

The development of bactericidal surfaces has gain traction in recent year due to fact that bacteria can develop resistance toward antibiotic [120]. COVID 19 pandemic has strengthened the need of anti-bacteria or anti-viral surfaces in our daily life. Bacterial infections start with bacteria attachment or adhesion to the surface of medical devices, hospital tools, implants, and food packaging. After bacterial attachment, bacteria will form biofilms, which is the formation that has high resistance against antibacterial agents[121], [122]. These material give preventive measure for infection by stopping adhesion of bacteria or virus

Contrary to antimicrobial application, cell-nanotopography interactions can be harness to create an environment that accelerate tissue repair and wound healing. Biologically inspired nanoscaffold and nanopattern has help researcher narrow down the pattern suitable for tissue repair and regeneration[123], [124]. With the comprehensive research and suitable fabrication for mass production, these biologically inspired nanoscaffold will have advances renegeraive medicine and tissue engineering. Many studies and research have been conducted to utilizes the biophysical cues from cell-substrate interaction for cardiovascular disease therapy. In vitro study show that when hESC-CMs (human embryonic stem cell-derived cardiomyocytes), in contact with nano- mirco surfaces will effect cardiomyocyte response[125], [126]. The cell morphology changes such as increase in alignment help regional cardiomyocyte which ultimately help the arrangement of cardiac muscle fiber[125], [126]. Cell reaction from nanotopographical cues also apparent in neural tissue regeneration and repair. Many bio-inspired nano-scaffolds are proven in helping for suitable environment for regeneration of various stem cell. Klymov et al. has reported that for neuron cell, PC12 show axonal growth in contact with nanogroovess with pitch 150-1000nm and depth 30-150nm[127]. Similar study by Genchi et al. show that PC12 cell adhesion and proliferation when in contact with 1μm random PHB fiber and parallel PHB fiber[127].

5. CONCLUSION AND PERSPECTIVES

In years after the cell first contact response, considerable progress has been made in establishing the fundamental of cell response to nanostructure. The future of cell-nanotopography interaction applications largely depends on advancement for high-throughput, cost effective nanofabrication techniques. Method such as nanoimprint lithography and electrospinning offer potential solutions of such applications.

Parallel developments in semiconductor industry, MEMs/NEMs and polymer research help tremendously for low cost cell-nanotopography-related devices. In the wake of COVID 19, applications like antimicrobial surfaces has create awareness for an pre-emptive approach from infections. The combinations of research for better nanofabrication, the demand for cell-nanotopographical applications and the continuous awareness campaign are hope to propel the nanotechnology implementation in health science.

AKNOWLEDGEMENT

This work was supported by the Universiti Sains Malaysia under USM Short Term (Grant No. 304 / PMEKANIK / 6315767).

REFERENCE

[1] M. A. Alghamdi, A. N. Fallica, N. Virzì, P. Kesharwani, V. Pittalà, and K. Greish, "The Promise of Nanotechnology in Personalized Medicine," *J. Pers. Med.*, vol. 12, no. 5, p. 673, 2022.

[2] R. Bosetti and S. L. Jones, "Cost–effectiveness of nanomedicine: estimating the real size of nano-costs," *Nanomedicine*, vol. 14, no. 11, pp. 1367–1370, 2019.

[3] B. A. Hemdan, G. K. Hassan, A. B. Abou Hammad, and A. M. El Nahrawy, "Industrial Perspective of Microbial Application of Nanoparticles Synthesis," in *Microbial Nanotechnology: Green Synthesis and Applications*, Springer, 2021, pp. 155–190.

[4] S. N. Joshi and P. Chandra, *Advanced Micro-and Nano-manufacturing Technologies: Applications in Biochemical and Biomedical Engineering*. Springer Nature, 2021.

[5] R. G. Harrison, "On the stereotropism of embryonic cells," *Science (80-.).*, vol. 34, no. 870, pp. 279–281, 1911.

[6] P. Weiss and B. Garber, "Shape and movement of mesenchyme cells as functions of the physical structure of the medium: contributions to a quantitative morphology," *Proc. Natl. Acad. Sci. U. S. A.*, vol. 38, no. 3, p. 264, 1952.

[7] C. J. Bettinger, R. Langer, and J. T. Borenstein, "Engineering substrate topography at the micro-and nanoscale to control cell function," *Angew. Chemie Int. Ed.*, vol. 48, no. 30, pp. 5406–5415, 2009.

[8] W. Chen *et al.*, "Nanotopography influences adhesion, spreading, and self-renewal of human embryonic stem cells," *ACS Nano*, vol. 6, no. 5, pp. 4094–4103, 2012.

[9] P. Friedl and E.-B. Bröker, "T cell migration in three-dimensional extracellular matrix: guidance by polarity and sensations," *Dev. Immunol.*, vol. 7, no. 2–4, pp. 249–266, 2000.

[10] J. Sutherland, M. Denyer, and S. Britland, "Contact guidance in human dermal fibroblasts is modulated by population pressure," *J. Anat.*, vol. 206, no. 6, pp. 581–587, 2005.

[11] P. Tsimbouri *et al.*, "Nanotopographical effects on mesenchymal stem cell morphology and phenotype," *J. Cell. Biochem.*, vol. 115, no. 2, pp. 380–390, 2014.

[12] K. Wolf, R. Müller, S. Borgmann, E.-B. Brocker, and P. Friedl, "Amoeboid shape change and contact guidance: T-lymphocyte crawling through fibrillar collagen is independent of matrix remodeling by MMPs and other proteases," *Blood*, vol. 102, no. 9, pp. 3262–3269, 2003.

[13] M. J. Dalby, N. Gadegaard, and R. O. C. Oreffo, "Harnessing nanotopography and integrin–matrix interactions to influence stem cell fate," *Nat. Mater.*, vol. 13, no. 6, pp. 558–569, 2014.

[14] J. O. Gallagher, K. F. McGhee, C. D. W. Wilkinson, and M. O. Riehle, "Interaction of animal cells with ordered nanotopography," *IEEE Trans. Nanobioscience*, vol. 99, no. 1, pp. 24–28, 2002.

[15] K. Lee, A. Mazare, and P. Schmuki, "One-dimensional titanium dioxide nanomaterials: nanotubes," *Chem. Rev.*, vol. 114, no. 19, pp. 9385–9454, 2014.

[16] K. Anselme, P. Davidson, A. M. Popa, M. Giazzon, M. Liley, and L. Ploux, "The interaction of cells and bacteria with surfaces structured at the nanometre scale," *Acta Biomater.*, vol. 6, no. 10, pp. 3824–3846, 2010.

[17] M. J. Dalby *et al.*, "The control of human mesenchymal cell differentiation using nanoscale symmetry and disorder," *Nat. Mater.*, vol. 6, no. 12, pp. 997–1003, 2007.

[18] J. Luo, M. Walker, Y. Xiao, H. Donnelly, M. J. Dalby, and M. Salmeron-Sanchez, "The influence of nanotopography on cell behaviour through interactions with the extracellular matrix–A review," *Bioact. Mater.*, 2021.

[19] Y. Cheng, G. Feng, and C. I. Moraru, "Micro-and nanotopography sensitive bacterial attachment mechanisms: a review," *Front. Microbiol.*, vol. 10, p. 191, 2019.

[20] S. Gupta, V. Krishnakumar, Y. Sharma, A. K. Dinda, and S. Mohanty, "Mesenchymal stem cell derived exosomes: a nano platform for therapeutics and drug delivery in combating COVID-19," *Stem cell Rev. reports*, vol. 17, no. 1, pp. 33–43, 2021.

[21] S. Kwon, K. H. Yoo, S. J. Sym, and D. Khang, "Mesenchymal stem cell therapy assisted by nanotechnology: a possible combinational treatment for brain tumor and central nerve regeneration," *Int. J. Nanomedicine*, vol. 14, p. 5925, 2019.

[22] J.-Y. Ko, H.-J. Oh, J. Lee, and G.-I. Im, "Nanotopographic influence on the in vitro behavior of induced pluripotent stem cells," *Tissue Eng. Part A*, vol. 24, no. 7–8, pp. 595–606, 2018.

[23] C. Zhao, X. Wang, L. Gao, L. Jing, Q. Zhou, and J. Chang, "The role of the micro-pattern and nano-topography of hydroxyapatite bioceramics on stimulating osteogenic differentiation of mesenchymal stem cells," *Acta Biomater.*, vol. 73, pp. 509–521, 2018.

[24] W. Ma, Y. Zhan, Y. Zhang, C. Mao, X. Xie, and Y. Lin, "The biological applications of DNA nanomaterials: current challenges and future directions," *Signal Transduct. Target. Ther.*, vol. 6, no. 1, pp. 1–28, 2021.

[25] L. N. West-Livingston, J. Park, S. J. Lee, A. Atala, and J. J. Yoo, "The role of the microenvironment in controlling the fate of bioprinted stem cells," *Chem. Rev.*, vol. 120, no. 19, pp. 11056–11092, 2020.

[26] G. Fytianos, A. Rahdar, and G. Z. Kyzas, "Nanomaterials in cosmetics: Recent updates," *Nanomaterials*, vol. 10, no. 5, p. 979, 2020.

[27] K. S. Beckwith, S. Ullmann, J. Vinje, and P. Sikorski, "Influence of nanopillar arrays on fibroblast motility, adhesion, and migration mechanisms," *Small*, vol. 15, no. 43, p. 1902514, 2019.

[28] S. Cai, C. Wu, W. Yang, W. Liang, H. Yu, and L. Liu, "Recent advance in surface modification for regulating cell adhesion and behaviors," *Nanotechnol. Rev.*, vol. 9, no. 1, pp. 971–989, 2020.

[29] D. Chopra, K. Gulati, and S. Ivanovski, "Understanding and optimizing the antibacterial functions of anodized nano-engineered titanium implants," *Acta Biomater.*, vol. 127, pp. 80–101, 2021.

[30] S. Spriano, S. Yamaguchi, F. Baino, and S. Ferraris, "A critical review of multifunctional titanium surfaces: New frontiers for improving osseointegration and host response, avoiding bacteria contamination," *Acta Biomater.*, vol. 79, pp. 1–22, 2018.

[31] A. Barlian and K. Vanya, "Nanotopography in directing osteogenic differentiation of mesenchymal stem cells: Potency and future perspective," *Futur. Sci. OA*, vol. 8, no. 1, p. FSO765, 2022.

[32] B. N. Kharbikar, P. Mohindra, and T. A. Desai, "Biomaterials to enhance stem cell transplantation," *Cell Stem Cell*, 2022.

[33] C. H. Choi, S. H. Hagvall, B. M. Wu, J. C. Dunn, R. E. Beygui, and C. J. K. CJ, "Cell interaction with three-dimensional sharp-tip nanotopography," *Biomaterials*, vol. 28, no. 9, pp. 1672–1679, 2007, doi: 10.1016/j.biomaterials.2006.11.031.

[34] M. J. Dalby, N. Gadegaard, M. O. Riehle, C. D. Wilkinson, and A. S. Curtis, "Investigating filopodia sensing using arrays of defined nano-pits down to 35 nm diameter in size," *Int J Biochem Cell Biol*, vol. 36, no. 10, pp. 2005–2015, 2004, doi: 10.1016/j.biocel.2004.03.001.

[35] T. Sjöström, M. J. Dalby, A. Hart, R. Tare, R. O. C. Oreffo, and B. Su, "Fabrication of pillar-like titania nanostructures on titanium and their interactions with human skeletal stem cells," *Acta Biomater*, vol. 5, no. 5, pp. 1433–1441, 2009, doi: http://dx.doi.org/10.1016/j.actbio.2009.01.007.

[36] R. M. Leven, A. S. Virdi, and D. R. Sumner, "Patterns of gene expression in rat bone marrow stromal cells cultured on titanium alloy discs of different roughness," *J Biomed Mater Res A*, vol. 70, no. 3, pp. 391–401, 2004, doi: 10.1002/jbm.a.30082.

[37] R. J. McMurray *et al.*, "Nanoscale surfaces for the long-term maintenance of mesenchymal stem cell phenotype and multipotency," *Nat. Mater.*, vol. 10, no. 8, pp. 637–644, 2011.

[38] T. Gong, J. Xie, J. Liao, T. Zhang, S. Lin, and Y. Lin, "Nanomaterials and bone regeneration," *Bone Res.*, vol. 3, no. 1, pp. 1–7, 2015.

[39] H. O. Ozguldez, J. Cha, Y. Hong, I. Koh, and P. Kim, "Nanoengineered, cell-derived extracellular matrix influences ECM-related gene expression of mesenchymal stem cells," *Biomater. Res.*, vol. 22, no. 1, pp. 1–9, 2018.

[40] Y. Yang, K. Wang, X. Gu, and K. W. Leong, "Biophysical regulation of cell behavior—cross talk between substrate stiffness and nanotopography," *Engineering*, vol. 3, no. 1, pp. 36–54, 2017.

[41] R. Muhammad, G. S. L. Peh, K. Adnan, J. B. K. Law, J. S. Mehta, and E. K. F. Yim, "Micro-and nano-topography to enhance proliferation and sustain functional markers of donor-derived primary human corneal endothelial cells," *Acta Biomater.*, vol. 19, pp. 138–148, 2015.

[42] S. Antonini *et al.*, "Human mesenchymal stromal cell-enhanced osteogenic differentiation by contact interaction with polyethylene terephthalate nanogratings," *Biomed. Mater.*, vol. 11, no. 4, p. 045003, 2016.

[43] H. Donnelly, M. J. Dalby, M. Salmeron-Sanchez, and P. E. Sweeten, "Current approaches for modulation of the nanoscale interface in the regulation of cell behavior," *Nanomedicine Nanotechnology, Biol. Med.*, vol. 14, no. 7, pp. 2455–2464, 2018.

[44] A. Murali, G. Lokhande, K. A. Deo, A. Brokesh, and A. K. Gaharwar, "Emerging 2D nanomaterials for biomedical applications," *Mater. Today*, vol. 50, pp. 276–302, 2021.

[45] Q. Zhou *et al.*, "Engineering aligned electrospun PLLA microfibers with nano-porous surface nanotopography for modulating the responses of vascular smooth muscle cells," *J. Mater. Chem. B*, vol. 3, no. 21, pp. 4439–4450, 2015.

[46] A. Lopez Marquez, I. E. Gareis, F. J. Dias, C. Gerhard, and M. F. Lezcano, "How Fiber Surface Topography Affects Interactions between Cells and Electrospun Scaffolds: A Systematic Review," *Polymers (Basel).*, vol. 14, no. 1, p. 209, 2022.

[47] R. M. Delaine-Smith, A. J. Hann, N. H. Green, and G. C. Reilly, "Electrospun Fiber Alignment Guides Osteogenesis and Matrix Organization Differentially in Two Different Osteogenic Cell Types," *Front. Bioeng. Biotechnol.*, vol. 9, 2021.

[48] W. Chen, Y. Sun, and J. Fu, "Microfabricated Nanotopological Surfaces for Study of Adhesion-Dependent Cell Mechanosensitivity," *Small*, vol. 9, no. 1, pp. 81–89, 2013.

[49] S. K. Stewart, "Fracture non-union: a review of clinical challenges and future research needs," *Malaysian Orthop. J.*, vol. 13, no. 2, p. 1, 2019.

[50] G. D. Pemberton *et al.*, "Nanoscale stimulation of osteoblastogenesis from mesenchymal stem cells: nanotopography and nanokicking," *Nanomedicine*, vol. 10, no. 4, pp. 547–560, 2015.

[51] Q. Sun, Y. Hou, Z. Chu, and Q. Wei, "Soft overcomes the hard: Flexible materials adapt to cell adhesion to promote cell mechanotransduction," *Bioact. Mater.*, vol. 10, pp. 397–404, 2022.

[52] R. Choe, E. Jabari, B. Mahadik, and J. Fisher, "3D Bioprinting and Nanotechnology for Bone Tissue Engineering," in *Bone Tissue Engineering*, Springer, 2022, pp. 193–223.

[53] S. Oh *et al.*, "Stem cell fate dictated solely by altered nanotube dimension," *Proc. Natl. Acad. Sci.*, vol. 106, no. 7, pp. 2130–2135, 2009.

[54] M. L. Nakamoto, C. Forró, W. Zhang, C.-T. Tsai, and B. Cui, "Expansion Microscopy for Imaging the Cell–Material Interface," *ACS Nano*, 2022.

[55] G. Joseph, R. P. Orme, T. Kyriacou, R. A. Fricker, and P. Roach, "Effects of Surface Chemistry Interaction on Primary Neural Stem Cell Neurosphere Responses," *ACS omega*, vol. 6, no. 30, pp. 19901–19910, 2021.

[56] M. Mirbagheri, V. Adibnia, B. R. Hughes, S. D. Waldman, X. Banquy, and D. K. Hwang, "Advanced cell culture platforms: a growing quest for emulating natural tissues," *Mater. Horizons*, vol. 6, no. 1, pp. 45–71, 2019.

[57] M. Ermis, E. Antmen, and V. Hasirci, "Micro and Nanofabrication methods to control cell-substrate interactions and cell behavior: A review from the tissue engineering perspective," *Bioact. Mater.*, vol. 3, no. 3, pp. 355–369, 2018.

[58] D. A. C. Walma and K. M. Yamada, "The extracellular matrix in development," *Development*, vol. 147, no. 10, p. dev175596, 2020.

[59] P. Kanchanawong *et al.*, "Nanoscale architecture of integrin-based cell adhesions," *Nature*, vol. 468, no. 7323, pp. 580–584, 2010.

[60] J.-L. Guan and D. Shalloway, "Regulation of focal adhesion-associated protein tyrosine kinase by both cellular adhesion and oncogenic transformation," *Nature*, vol. 358, no. 6388, pp. 690–692, 1992.

[61] J.-L. Guan, J. E. Trevithick, and R. O. Hynes, "Fibronectin/integrin interaction induces tyrosine phosphorylation of a 120-kDa protein.," *Cell Regul.*, vol. 2, no. 11, pp. 951–964, 1991.

[62] C. González-García, M. Salmerón-Sánchez, and A. J. García, "Focal Adhesion Kinase in Cell–Material Interactions," *Polym. Regen. Med. Biomed. Appl. from Nano-to Macro-Structures*, pp. 147–176, 2015.

[63] S. K. Mitra, D. A. Hanson, and D. D. Schlaepfer, "Focal adhesion kinase: in command and control of cell motility," *Nat Rev Mol Cell Biol*, vol. 6, no. 1, pp. 56–68, 2005, doi: 10.1038/nrm1549.

[64] M. J. Kratochvil, A. J. Seymour, T. L. Li, S. P. Paşca, C. J. Kuo, and S. C. Heilshorn, "Engineered materials for organoid systems," *Nat. Rev. Mater.*, vol. 4, no. 9, pp. 606–622, 2019.

[65] D. P. Linklater, V. A. Baulin, S. Juodkazis, R. J. Crawford, P. Stoodley, and E. P. Ivanova, "Mechano-bactericidal actions of nanostructured surfaces," *Nat. Rev. Microbiol.*, vol. 19, no. 1, pp. 8–22, 2021.

[66] M. Rahmati, E. A. Silva, J. E. Reseland, C. A. Heyward, and H. J. Haugen, "Biological responses to physicochemical properties of biomaterial surface," *Chem. Soc. Rev.*, vol. 49, no. 15, pp. 5178–5224, 2020.

[67] E. A. Cavalcanti-Adam, D. Aydin, V. C. Hirschfeld-Warneken, and J. P. Spatz, "Cell adhesion and response to synthetic nanopatterned environments by steering receptor clustering and spatial location," *HFSP J.*, vol. 2, no. 5, pp. 276–285, 2008.

[68] J. Kim *et al.*, "Synergistic effects of nanotopography and co-culture with endothelial cells on osteogenesis of mesenchymal stem cells," *Biomaterials*, vol. 34, no. 30, pp. 7257–7268, 2013.

[69] K. Y. Lee *et al.*, "Nanoscale adhesion ligand organization regulates osteoblast proliferation and differentiation," *Nano Lett.*, vol. 4, no. 8, pp. 1501–1506, 2004.

[70] K. Poole *et al.*, "Molecular-scale topographic cues induce the orientation and directional movement of fibroblasts on two-dimensional collagen surfaces," *J. Mol. Biol.*, vol. 349, no. 2, pp. 380–386, 2005.

[71] C. Vieu *et al.*, "Electron beam lithography: resolution limits and applications," *Appl. Surf. Sci.*, vol. 164, no. 1–4, pp. 111–117, 2000.

[72] L. Liu, Y. Zhang, W. Wang, C. Gu, X. Bai, and E. Wang, "Nanosphere Lithography for the Fabrication of Ultranarrow Graphene Nanoribbons and On-Chip Bandgap Tuning of Graphene," *Adv. Mater.*, vol. 23, no. 10, pp. 1246–1251, Mar. 2011, doi: 10.1002/adma.201003847.

[73] K. Mohamed, "Three-Dimensional Patterning Using Ultraviolet Curable Nanoimprint Lithography.," 2009.

[74] A. H. A. Manap and K. Mohamed, "Molecular dynamics simulation on selective etching of α-quartz and amorphous quartz substrate using low-energy argon ion bombardment model in dry etching process," vol. 14, no., p. 33505, 2015, [Online]. Available: https://doi.org/10.1117/1.JMM.14.3.033505

[75] A. Schleunitz, C. Spreu, T. Mäkelä, T. Haatainen, A. Klukowska, and H. Schift, "Hybrid working stamps for high speed roll-to-roll nanoreplication with molded sol–gel relief on a metal backbone," *Microelectron. Eng.*, vol. 88, no. 8, pp. 2113–2116, 2011, doi: https://doi.org/10.1016/j.mee.2011.02.019.

[76] S. Y. Chou, P. R. Krauss, and P. J. Renstrom, "Imprint of sub-25 nm vias and trenches in polymers," *Appl. Phys. Lett.*, vol. 67, no. 21, pp. 3114–3116, Nov. 1995, doi: 10.1063/1.114851.

[77] A. H. Abdul Manap, S. S. Md Izah, and K. Mohamed, "Molecular Dynamics Study of Poly (dimethylsiloxane) Nanostructure Distortion in a Soft Lithography Demolding Process," *ACS omega*, vol. 4, no. 23, pp. 20257–20264, 2019.

[78] A. H. Abdul Manap, L. Shamsuddin, and K. Mohamed, "The study of polydimethylsiloxane nanocone distortion in the demolding process using molecular dynamics method," *AIP Adv.*, vol. 12, no. 4, p. 45011, 2022.

[79] A. M. Al-Dhahebi *et al.*, "Electrospinning research and products: The road and the way forward," *Appl. Phys. Rev.*, vol. 9, no. 1, p. 11319, 2022.

[80] K. Raj M and S. Chakraborty, "PDMS microfluidics: A mini review," *J. Appl. Polym. Sci.*, vol. 137, no. 27, p. 48958, 2020.

[81] M. M. Alkaisi and K. Mohamed, "Three-dimensional patterning using ultraviolet nanoimprint lithography," in *Lithography*, IntechOpen, 2010.

[82] M. Colburn *et al.*, "Step and flash imprint lithography: a new approach to high-resolution patterning," in *Emerging Lithographic Technologies III*, 1999, vol. 3676, pp. 379–389. doi: 10.1117/12.351155.

[83] J. Lee, S. Park, K. Choi, and G. Kim, "Nano-scale patterning using the roll typed UV-nanoimprint lithography tool," *Microelectron. Eng.*, vol. 85, no. 5, pp. 861–865, 2008, doi: https://doi.org/10.1016/j.mee.2007.12.059.

[84] M. Vogler *et al.*, "Development of a novel, low-viscosity UV-curable polymer system for UV-nanoimprint lithography," *Microelectron. Eng.*, vol. 84, no. 5, pp. 984–988, 2007, doi: https://doi.org/10.1016/j.mee.2007.01.184.

[85] P. C. Sousa *et al.*, "Nanoimprint lithography for large-scale fabrication of micro-and nano-structures".

[86] E. H. Ahn *et al.*, "Spatial control of adult stem cell fate using nanotopographic cues," *Biomaterials*, vol. 35, no. 8, pp. 2401–2410, 2014.

[87] S. Lan, H. Lee, J. Ni, S. Lee, and M. Lee, "Survey on roller-type nanoimprint lithography (RNIL) process," in *2008 International Conference on Smart Manufacturing Application*, 2008, pp. 371–376.

[88] H. Lan, "Large-Area nanoimprint lithography and applications," *Micro/Nanolithography-A heuristic Asp. Endur. Technol.*, pp. 43–68, 2018.

[89] H. C. Wong, G. Grenci, J. Wu, V. Viasnoff, and H. Y. Low, "Roll-to-roll fabrication of residual-layer-free micro/nanoscale membranes with precise pore architectures and tunable surface textures," *Ind. Eng. Chem. Res.*, vol. 57, no. 41, pp. 13759–13768, 2018.

[90] Y. Chen *et al.*, "Sub-10 nm fabrication: methods and applications," *Int. J. Extrem. Manuf.*, vol. 3, no. 3, p. 32002, 2021.

[91] D. Ye *et al.*, "UV nanoimprint lithography of sub-100nm nanostructures using a novel UV curable epoxy siloxane polymer," *Microelectron. Eng.*, vol. 87, no. 11, pp. 2411–2415, 2010, doi: https://doi.org/10.1016/j.mee.2010.04.016.

[92] S. S. Deshmukh and A. Goswami, "Current innovations in roller embossing—A comprehensive review," *Microsyst. Technol.*, pp. 1–38, 2022.

[93] K. Nagato, S. Sugimoto, T. Hamaguchi, and M. Nakao, "Iterative roller imprint of multilayered nanostructures," *Microelectron. Eng.*, vol. 87, no. 5–8, pp. 1543–1545, 2010.

[94] S. H. Lee, S. W. Kim, B. S. Kang, P.-S. Chang, and M. K. Kwak, "Scalable and continuous fabrication of bio-inspired dry adhesives with a thermosetting polymer," *Soft Matter*, vol. 14, no. 14, pp. 2586–2593, 2018.

[95] Y. Wang, X. Zhao, X. Jiao, and D. Chen, "Electrospun filters for air filtration: comparison with existing air filtration technologies," in *Filtering Media by Electrospinning*, Springer, 2018, pp. 47–67.

[96] I. G. Kim, J.-H. Lee, A. R. Unnithan, C.-H. Park, and C. S. Kim, "A comprehensive electric field analysis of cylinder-type multi-nozzle electrospinning system for mass production of nanofibers," *J. Ind. Eng. Chem.*, vol. 31, pp. 251–256, 2015.

[97] M. D. Rosenberg, "Cell guidance by alterations in monomolecular films," *Science (80-.).*, vol. 139, no. 3553, pp. 411–412, 1963.

[98] C. T. Laurencin, A. M. A. Ambrosio, M. D. Borden, and J. A. Cooper Jr, "Tissue engineering: orthopedic applications," *Annu. Rev. Biomed. Eng.*, vol. 1, no. 1, pp. 19–46, 1999.

[99] A. Formhals, "United States: Patent Application Publication," *US Pat.*, vol. 1, no. 1934, p. 504, 1934.
[100] F. N. H. Karabulut, G. Höfler, N. Ashok Chand, and G. W. Beckermann, "Electrospun Nanofibre Filtration Media to Protect against Biological or Nonbiological Airborne Particles," *Polymers (Basel).*, vol. 13, no. 19, p. 3257, 2021.
[101] W. Yu *et al.*, "A novel electrospun nerve conduit enhanced by carbon nanotubes for peripheral nerve regeneration," *Nanotechnology*, vol. 25, no. 16, p. 165102, 2014.
[102] B. Zhu, W. Li, R. V Lewis, C. U. Segre, and R. Wang, "E-spun composite fibers of collagen and dragline silk protein: fiber mechanics, biocompatibility, and application in stem cell differentiation," *Biomacromolecules*, vol. 16, no. 1, pp. 202–213, 2015.
[103] M. Cho, S.-H. Kim, G. Jin, K. I. Park, and J.-H. Jang, "Salt-induced electrospun patterned bundled fibers for spatially regulating cellular responses," *ACS Appl. Mater. Interfaces*, vol. 8, no. 21, pp. 13320–13331, 2016.
[104] C. D. L. Johnson, A. R. D'Amato, and R. J. Gilbert, "Electrospun fibers for drug delivery after spinal cord injury and the effects of drug incorporation on fiber properties," *Cells Tissues Organs*, vol. 202, no. 1–2, pp. 116–135, 2016.
[105] J. A. Roman, I. Reucroft, R. A. Martin, A. Hurtado, and H. Mao, "Local release of paclitaxel from aligned, electrospun microfibers promotes axonal extension," *Adv. Healthc. Mater.*, vol. 5, no. 20, pp. 2628–2635, 2016.
[106] S. Shafei, J. Foroughi, L. Stevens, C. S. Wong, O. Zabihi, and M. Naebe, "Electroactive nanostructured scaffold produced by controlled deposition of PPy on electrospun PCL fibres," *Res. Chem. Intermed.*, vol. 43, no. 2, pp. 1235–1251, 2017.
[107] E. P. Ivanova *et al.*, "Bactericidal activity of black silicon," *Nat. Commun.*, vol. 4, no. 1, pp. 1–7, 2013.
[108] G. S. Watson *et al.*, "A gecko skin micro/nano structure–A low adhesion, superhydrophobic, anti-wetting, self-cleaning, biocompatible, antibacterial surface," *Acta Biomater.*, vol. 21, pp. 109–122, 2015.
[109] S. M. Kelleher *et al.*, "Cicada wing surface topography: an investigation into the bactericidal properties of nanostructural features," *ACS Appl. Mater. Interfaces*, vol. 8, no. 24, pp. 14966–14974, 2016.
[110] J. Hasan, S. Raj, L. Yadav, and K. Chatterjee, "Engineering a nanostructured 'super surface' superhydrophobic and superkilling properties †," *RSC Adv.*, vol. 5, pp. 44953–44959, 2015, doi: 10.1039/c5ra05206h.
[111] L. E. Fisher *et al.*, "Bactericidal activity of biomimetic diamond nanocone surfaces Bactericidal activity of biomimetic diamond nanocone surfaces," *Biointerphases*, vol. 011014, 2016, doi: 10.1116/1.4944062.
[112] P. W. May *et al.*, "Diamond-coated 'black silicon' as promising material for high-surface-area electrochemical electrodes and antibacterial surfaces," *J. Mater. Chem. B*, vol. 4, pp. 5737–5746, 2016, doi: 10.1039/c6tb01774f.
[113] C. M. Bhadra *et al.*, "Antibacterial titanium nano-patterned arrays inspired by dragonfly wings," *Nat. Publ. Gr.*, pp. 1–12, 2015, doi: 10.1038/srep16817.
[114] F. Hizal, I. Zhuk, S. Sukhishvili, H. j Busscher, H. C. Van Der Mei, and C. Choi, "Impact of 3D Hierarchical Nanostructures on the Antibacterial Efficacy of a Bacteria-Triggered Self-Defensive Antibiotic Coating," *ACS Appl. Mater. Interfaces*, vol. 7, pp. 20304–20313, 2015, doi: 10.1021/acsami.5b05947.
[115] T. Sjöström, A. H. Nobbs, and B. Su, "Bactericidal nanospike surfaces via thermal oxidation of Ti alloy substrates," *Mater. Lett.*, vol. 167, pp. 22–26, 2016, doi: 10.1016/j.matlet.2015.12.140.
[116] M. N. Dickson, E. I. Liang, L. A. Rodriguez, N. Vollereaux, and A. F. Yee, "Nanopatterned polymer surfaces with bactericidal properties," *Biointerphases*, vol. 10, no. June, pp. 1–8, 2015, doi: 10.1116/1.4922157.
[117] S. Kim *et al.*, "Nanostructured Multifunctional Surface with Antire fl ective and Antimicrobial Characteristics," *ACS Appl. Mater. Interfaces*, 2015, doi: 10.1021/am506254r.
[118] J. Valle *et al.*, "Evaluation of Surface Microtopography Engineered by Direct Laser Interference for Bacterial Anti-Biofouling a," *Macromol. Biosci.*, vol. 15, pp. 1060–1069, 2015, doi: 10.1002/mabi.201500107.
[119] N. Lu, W. Zhang, Y. Weng, X. Chen, Y. Cheng, and P. Zhou, "Fabrication of PDMS surfaces with micro patterns and the effect of pattern sizes on bacteria adhesion," *Food Control*, vol. 68, pp. 344–351, 2016, doi: 10.1016/j.foodcont.2016.04.014.
[120] A. Gupta, S. Mumtaz, C.-H. Li, I. Hussain, and V. M. Rotello, "Combatting antibiotic-resistant bacteria using nanomaterials," *Chem. Soc. Rev.*, vol. 48, no. 2, pp. 415–427, 2019.
[121] F. Liu, P. Jin, H. Gong, Z. Sun, L. Du, and D. Wang, "Antibacterial and antibiofilm activities of thyme oil against foodborne multiple antibiotics-resistant Enterococcus faecalis," *Poult. Sci.*, vol. 99, no. 10, pp. 5127–5136, 2020.
[122] P. Angelopoulou, E. Giaouris, and K. Gardikis, "Applications and Prospects of Nanotechnology in Food and Cosmetics Preservation," *Nanomaterials*, vol. 12, no. 7, p. 1196, 2022.
[123] G. Funda *et al.*, "Nanotechnology scaffolds for alveolar bone regeneration," *Materials (Basel).*, vol. 13, no. 1, p. 201, 2020.
[124] S. Chen, R. Li, X. Li, and J. Xie, "Electrospinning: An enabling nanotechnology platform for drug delivery and regenerative medicine," *Adv. Drug Deliv. Rev.*, vol. 132, pp. 188–213, 2018.

[125] J. H. Tsui *et al.*, "Conductive silk–polypyrrole composite scaffolds with bioinspired nanotopographic cues for cardiac tissue engineering," *J. Mater. Chem. B*, vol. 6, no. 44, pp. 7185–7196, 2018.
[126] A. Chen *et al.*, "Integrated platform for functional monitoring of biomimetic heart sheets derived from human pluripotent stem cells," *Biomaterials*, vol. 35, no. 2, pp. 675–683, 2014.
[127] A. Klymov *et al.*, "Nanogrooved Surface-Patterns induce cellular organization and axonal outgrowth in neuron-like PC12-Cells," *Hear. Res.*, vol. 320, pp. 11–17, 2015.